

Simultaneous relaxometry and susceptibility imaging in the brain

Cheng-Chieh Cheng^{1,2}, Tzu-Cheng Chao³, Hsiao-Wen Chung¹, Lawrence Panych², and Bruno Madore²

¹Graduate Institute of Biomedical Electronics and Bioinformatics, National Taiwan University, Taipei, Taiwan, ²Radiology, Brigham and Women's Hospital, Harvard Medical School, Boston, MA, United States, ³Department of Computer Science and Information Engineering, National Cheng-Kung University, Tainan, Taiwan

Target Audience: Researchers interested in exploiting susceptibility imaging and relaxometry (T_2 and T_2^*) to detect and characterize disease states.

Purpose: Brain iron concentration and iron accumulation are of vast clinical interest for they may be related to brain diseases such as Parkinson's disease, Alzheimer's diseases, and multiple sclerosis. Iron content can be characterized through either susceptibility or relaxation rate measurements [1-3]. A novel imaging method is presented here that enables susceptibility imaging, T_2 and T_2^* mapping to be performed from a single rapid scan.

Theory: As in the 'dual echo steady-state' (DESS) sequence, two different types of signals are sampled during readout: an FID-like (S^+) and a spin echo-like (S^-) signal. Both signals are sampled at a few different TE locations, leading to a dual-pathway multi-echo sequence similar to the GESFIDE [4] sequence. A main development here involves generating quantitative T_2 and T_2^* maps from the resulting images. The relaxation of the sampled magnetization is described as:

$$\begin{aligned} |S^+| &\propto \exp[-TE \times (R_2 + R_2')] & Eq.1 \\ |S^-| &\propto \exp[-TR \times (R_2 + R_2')] \times \exp[-TE \times (R_2 - R_2')] & Eq.2 \end{aligned}$$

where R_2 and R_2' represent irreversible and reversible decay, respectively, such that $T_2 = 1/R_2$ and $T_2^* = 1/(R_2 + R_2')$. Because the S^- signal is similar to a spin-echo on its way to formation, reversible decay is in the process of being corrected and results in the $(R_2 - R_2')$ factor in the second term of Eq. 2. In contrast, $(R_2 + R_2')$ appears in Eq. 1, allowing the two variables to be separated and quantitative T_2 and T_2^* values to be calculated.

While Eqs. 1 and 2 involve the magnitude of S^+ and S^- and can be used for T_2 and T_2^* mapping, the phase of S^+ and S^- proves to be very-well suited for susceptibility imaging [5]. Because the S^- signal is rephasing towards an echo rather than dephasing away from excitation, it essentially doubles the range of TE values available for field mapping compared to a regular GRE sequence (by allowing both negative and positive TE values). For this reason, having both S^+ and S^- signals may have SNR advantages in the resulting field map and susceptibility-weighted images. Both signal intensity (S.I.) and phase evolutions are illustrated in Fig. 1.

Materials and Methods: Simulations were performed to optimize the scanning parameters (e.g., Fig. 2a). Assuming $T_1/T_2/T_2^* = 1500/100/60$ ms, TR and flip angle values were found that maximized the SNR efficiency in the calculated field maps, and values of TR = 50 ms and flip angle = 25 degrees were selected here. Four healthy volunteers were imaged (Siemens Trio, 3 T, 32-ch head matrix), with informed consent from an IRB-approved protocol. As shown in Fig. 1, four different echo times were sampled (TE = 7.1, 19.0, 31.0, and 42.9 ms, bandwidth = 110 Hz/px, matrix size = 192x192x36, voxel size = 1x1x2 mm³, total scan time = 5:47). For field mapping, BET and PRELUDE (FSL, Oxford, UK) [6] were used for brain extraction and phase unwrapping, and a spherical mean value method [7] was adopted to filter out external field perturbations. Using the signal magnitude, Eqs. 1 and 2 were solved for R_2 and R_2' . Six regions (white matter, caudate nucleus, putamen, globus pallidus, red nucleus, and substantia nigra) were contoured to evaluate the T_2 and T_2^* results.

Results and Discussion: Results for the internal field B_{int} , R_2 and $R_2^* = R_2 + R_2'$ are shown in Fig. 2 (b-d). The measured R_2 and R_2^* values are listed in Table 1 for various brain structures, along with the corresponding T_2 and T_2^* values. The measurements in Table 1 are in good agreement with findings from previous studies [8, 9]. In a scan time of less than 6 minutes, the proposed approach proved capable of generating good quality B_{int} , T_2 and T_2^* measurements over a 192x192x36 3D volume. These measurements are expected to prove useful in the detection and quantification of iron content, a condition that has been linked with research-intensive conditions such as Parkinson's disease, Alzheimer's diseases and multiple sclerosis. Scan time could be further reduced by including parallel imaging.

Conclusion: The proposed method is capable of simultaneously measuring R_2 , R_2' and the internal field perturbation from a single rapid scan.

References: [1] Haacke et al. *MRI* 2005;23:1-25. [2] Langkammer et al. *Radiology* 2010;257(2):455-62. [3] Langkammer et al. *NeuroImage* 2012;62:1593-9. [4] Ma, Wehrli. *JMR B*, 1996;111:61-9 [5] Cheng et al. *ISMRM* 2012, p. 2371. [6] Jenkinson et al. *Neuroimage* 2012;62:782-90. [7] Li, Leigh. *JMR* 2001;148(2):422-8. [8] Ordidge et al. *MRM* 1994;32:355-41. [9] Gelman et al. *Radiology* 1999;210:759-67. Acknowledged support from grants R01CA149342, R01EB010195, P41EB015898.

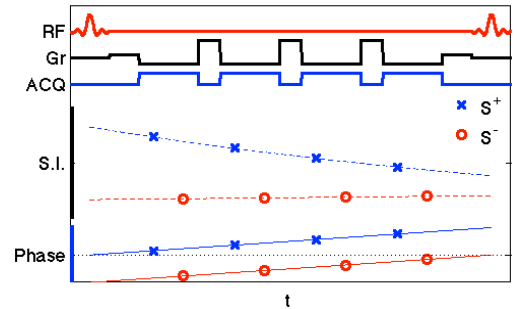


Figure 1: (Top) Sketch plot of our dual-pathway multi-echo steady-state sequence. (Middle) The blue and red dashed curves represent the evolution of $|S^+|$ and $|S^-|$, respectively. (Bottom) The blue and red solid lines represent the phase evolution of $|S^+|$ and $|S^-|$, respectively. Blue crosses and red circles indicate when gradient echoes are formed.

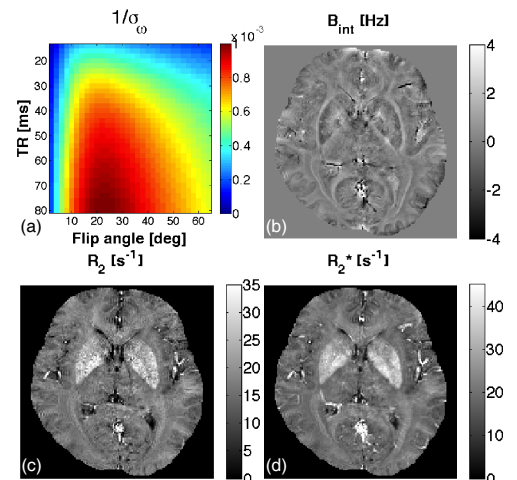


Figure 2: (a) Simulated SNR_0 derived from the variance of fitted frequency. (b) B_{int} map. (c) R_2 map. (d) R_2^* map.

Tissue	R_2 (s ⁻¹)	R_2^* (s ⁻¹)	T_2 (ms)	T_2^* (ms)
WM	17.5 ± 2.0	20.9 ± 2.2	57.0	47.8
CA	19.4 ± 4.5	25.8 ± 5.0	51.5	38.7
PUT	25.0 ± 4.7	32.2 ± 4.8	40.0	31.1
GP	27.6 ± 6.7	37.4 ± 4.8	36.3	26.8
RN	21.5 ± 5.3	29.5 ± 3.5	46.6	33.9
SN	22.4 ± 6.7	31.8 ± 4.9	44.7	31.4

Table 1: ROI analysis on relaxation rates and the corresponding relaxation times. (Mean ± S.D.)

(abbr: WM, white matter; CA, caudate nucleus; PUT, putamen; GP, globus pallidus; RN, red nucleus; SN, substantia nigra)